Clinical Neurophysiology 130 (2019) 1375–1386

Contents lists available at ScienceDirect

Clinical Neurophysiology

journal homepage: www.elsevier.com/locate/clinph

EEG-correlated fMRI of human alpha (de-)synchronization

Paul Knaut [a,*], Frederic von Wegner [a], Astrid Morzelewski [a], Helmut Laufs [a,b]

[a] Department of Neurology and Brain Imaging Center, Goethe University Frankfurt, Schleusenweg 2-16, 60528 Frankfurt am Main, Germany
[b] Department of Neurology, Christian-Albrechts-University Kiel, Arnold-Heller-Str. 3, Haus 41, 24105 Kiel, Germany

ARTICLE INFO

Article history:
Accepted 19 April 2019
Available online 24 May 2019

Keywords:
Simultaneous EEG-fMRI
Alpha rhythm
Sleep
Thalamus
Hippocampus
Memory

HIGHLIGHTS

- During wakefulness, light sleep (N1) intrusions occur and evade clinical sleep scoring rules.
- N1-induced drops in posterior EEG alpha power correlate with thalamic activity.
- Spatial-spectral EEG features track hippocampal BOLD-fMRI activity changes in N1.

ABSTRACT

Objectives: We investigated blood oxygenation level-dependent (BOLD) brain activity changes in wakefulness and light sleep and in relation to those associated with the posterior alpha rhythm, the most prominent feature of the clinical EEG. Studies have reported different sets of brain regions changing their oxygen consumption with waxing and waning alpha oscillations. Here, we hypothesize that these dissimilar activity patterns reflect different wakefulness-dependent brain states.
Methods: We recorded BOLD signal changes and electroencephalography (EEG) simultaneously in 149 subjects at rest. Based on American Academy of Sleep Medicine criteria, we selected subjects exhibiting wakefulness or light sleep (N1). We identified brain regions in which BOLD signal changes correlated with (i) clinical sleep stages, (ii) alpha band power and (iii) a multispectral EEG index, respectively.
Results: During light sleep, we found increased BOLD activity in parieto-occipital regions. In wakefulness compared to light sleep, we revealed BOLD signal increases in the thalamus. The multispectral EEG-index revealed hippocampal activity changes in light sleep not reported before.
Conclusion: Changes in alpha oscillations reflect different brain states associated with different levels of wakefulness and thalamic activity. We can link the previously described parieto-occipital pattern to drowsiness. Additionally, in that stage, we identify hippocampal activity fluctuations.
Significance: Thalamic activity varies with early changes of wakefulness, which is important to consider in resting state experiments. The EEG-indexed activation of the hippocampus during light sleep suggests that memory encoding might already take place during this early stage of sleep.

1. Introduction

Clinical electroencephalogram (EEG) is classically recorded during relaxed wakefulness with closed eyes. This condition evokes the unmistakable alpha rhythm, a mostly occipital 8–12 per second oscillation. Despite obvious external stimulation, alpha oscillations wax and wane seemingly spontaneously. What do alterations in alpha power indicate? Hans Berger first observed this rhythm and its reactivity to mental activity and sleep (Berger, 1929). Alpha function is still a matter of discussion: some consider it an 'idling rhythm' (Pfurtscheller et al., 1996), i.e. reflecting task-free cortical activity which is ready to react at any time. In contrast, Jensen and Mazaheri proposed a 'gating function', i.e. that alpha synchronization results from an active process inhibiting regions unconnected to an ongoing task (Jensen and Mazaheri, 2010). During drowsiness, posterior alpha oscillations fade and relocate to more frontal brain regions, and the EEG power of delta (0.5–4 Hz) and theta (4–8 Hz) frequencies increase (AASM, 2007).

The identification of blood oxygen level-dependent (BOLD) functional magnetic resonance imaging (fMRI) correlates of the alpha rhythm during task-free rest has attracted much attention. Correlations between alpha band power and the BOLD signal interrelated positively with BOLD signal changes in the thalamus and the

* Corresponding author.
E-mail address: paul.knaut@gmail.com (P. Knaut).

https://doi.org/10.1016/j.clinph.2019.04.715
1388-2457/

anterior cingulate cortex (Goldman et al., 2002; Feige et al., 2005; Difrancesco et al., 2008). These findings are in agreement with alpha rhythm models of thalamo-cortical circuits (Lopes da Silva et al., 1974; Valdes et al., 1999). Negative EEG-fMRI correlations showed equivocal results: while some studies found an occipital fMRI activation pattern (Goldman et al., 2002; Moosmann et al., 2003; Laufs et al., 2006) with reduced alpha oscillations, another study additionally revealed a bilateral fronto-parietal "deactivation" pattern (Laufs et al., 2003a). How can we explain these seemingly contradictory findings? The occipital pattern correlated positively with high theta power and negatively with beta power - compatible with an associated brain state of drowsiness (Laufs et al., 2006). Similarly, an analysis of BOLD signal changes during explicit states of reduced vigilance also yielded an occipital increase in BOLD activity (Olbrich et al., 2009). The fronto-parietal BOLD signal pattern associated with decreased EEG alpha power, however, was associated with high beta power and low theta power suggesting an "active" brain state during alpha blocking characterized by activity in attention sustaining brain regions (Laufs et al., 2006). Despite this indirect evidence, the hypothesis that the different alpha-associated BOLD signal patterns are actually due to different brain states remains to be put to test explicitly. Furthermore, not any study as of yet has investigated BOLD signal changes in response to amplitude fluctuations of alpha oscillations (alpha modulation) during relatively fast switches between wakefulness and drowsiness as defined by gold standard clinical sleep scoring (AASM, 2007) and often observed in the clinical EEG laboratory.

Here, we hypothesize that alpha desynchronization – obvious to the clinician's eyes - occurs during different brain states and that these can be differentiated by analysis of oscillatory EEG activity in frequency bands flanking alpha. Therefore, with simultaneous EEG and fMRI recordings we examined the BOLD signal changes in awake subjects and those transitioning between wakefulness and light sleep correlated both with the EEG alpha band power and parameters characterising this transition independently of alpha oscillations. We tested the hypothesis that BOLD-fMRI correlates of the EEG alpha rhythm depend on the state of wakefulness, and we explored which brain regions change their activity during the transition from wakefulness to light sleep. To achieve our goals, we extended clinically established sleep scoring, especially its temporal resolution.

2. Methods

2.1. Subjects

We recruited 149 non sleep-deprived individuals (87 female, age range 19–51 years, mean 25 years, standard deviation 4.8 years) whose neurological, psychiatric and cardiovascular medical history was unremarkable. Subjects were interviewed by doctors experienced in sleep medicine assessing sleep behaviour, medical disorders and medication. A sleep record covering the week preceding the experiment was obtained. Subjects with mental disorders, physical disorders or taking medication affecting wakefulness were excluded, equally those exhibiting an irregular sleep pattern, sleep deprivation or scoring nine and up on the Epworth sleepiness scale (Johns, 1991). We obtained the subjects' written informed consent (Goethe University ethics approval 305/07).

2.2. EEG and fMRI-acquisition

The subjects were scanned on weekdays in the evening between 8 and 9 pm. Subjects were instructed to lie still, relax and keep their eyes shut.

We recorded EEG via a cap (modified BrainCapMR, Easycap, Herrsching, Germany) continuously with fMRI (1505 volumes of $T2^*$-weighted echo planar images, TR/TE = 2080 ms/30 ms, matrix 64×64, voxel size $3 \times 3 \times 2\ mm^3$, distance factor 50%; FOV 192 mm^2, 32 slices acquired, equal inter-slice and inter-volume gaps) at 3 T (Siemens Trio, Erlangen, Germany) over 52 minutes with an optimized polysomnographic setting (chin and tibial EMG, ECG, EOG recorded bipolarly [sampling rate 5 kHz, low pass filter 250 Hz], and pulse oximetry, respiration recorded via sensors from the Trio [sampling rate 50 Hz]) using MR scanner compatible devices (BrainAmp MR+, BrainAmp ExG; Brain Products, Gilching, Germany) facilitating sleep scoring during fMRI acquisition (AASM, 2007; Laufs et al., 2007; Jahnke et al., 2012). Specifically, the EEG cap had 29 EEG electrodes positioned according to the international 10–10 system including F3/F4, C3/C4 and O1/O2. These were referenced offline to the contralateral mastoid electrode (TP9, TP10, respectively) and included in the montage used for sleep staging according to AASM recommendations (AASM, 2007).

2.3. EEG sleep scoring

An expert (AM) in sleep scoring performed sleep staging of the EEG data (52 minutes long, cf. "EEG and fMRI-acquisition) following the rules published by the American Academy of Sleep Medicine (AASM, 2007).

We excluded subjects if they exhibited any sleep stage deeper than N1 (light sleep). We divided the remaining 39 subjects into two groups (Fig. 1).

In Group 1 ("W/N1"), we included all subjects who reached sleep stage N1 (light sleep) during the simultaneous EEG-fMRI recording but did not enter any deeper sleep stages. In other words, they exclusively exhibited epochs of wakefulness (W) and epochs of drowsiness (N1). This resulted in 25 subjects (15 female, age range 20–48 years, mean 26 years).

In Group 2a ("W only"), we included all subjects who remained awake – i.e. exhibited exclusively epochs scored as wakefulness (W) throughout the recording. This resulted in 14 subjects (7 female, age 22–36 years, mean 26 years).

We also formed and analysed a Group 2b: Subjects fulfilling the AASM criteria for wakefulness during the recording time can still exhibit slight indications of drowsiness (at a time scale below 30 s), i.e. 4–7 Hz theta frequencies (Laufs et al., 2006). Based on this notion, an expert in EEG sleep scoring examined the data for such subtle indicators of drowsiness. Consequently, eight subjects remained who displayed hardly any signs of drowsiness and which formed Group 2b (3 female, age 22–29 years, mean 28 years, see Supplementary Table S2 for more details).

2.4. MRI and pulse artefact correction on the EEG

MRI and pulse artefact correction were performed based on the average artefact subtraction (AAS) method (Allen et al., 1998) as implemented in Vision Analyzer2 (Brain Products, Germany) followed by objective (CBC parameters, Vision Analyzer) ICA-based rejection of residual artefact-laden components after AAS (Jahnke et al., 2012) resulting in EEG with a sampling rate of 250 Hz.

2.5. Power spectral densities in Group 1 (W/N1)

To determine the frequency content of wake (W) and light sleep (N1) stages, as defined by the AASM rules, we analysed the 25 subjects, which exclusively showed W and N1 segments (for power spectral densities of pure wakefulness see Fig. S3 in von Wegner et al., 2016).

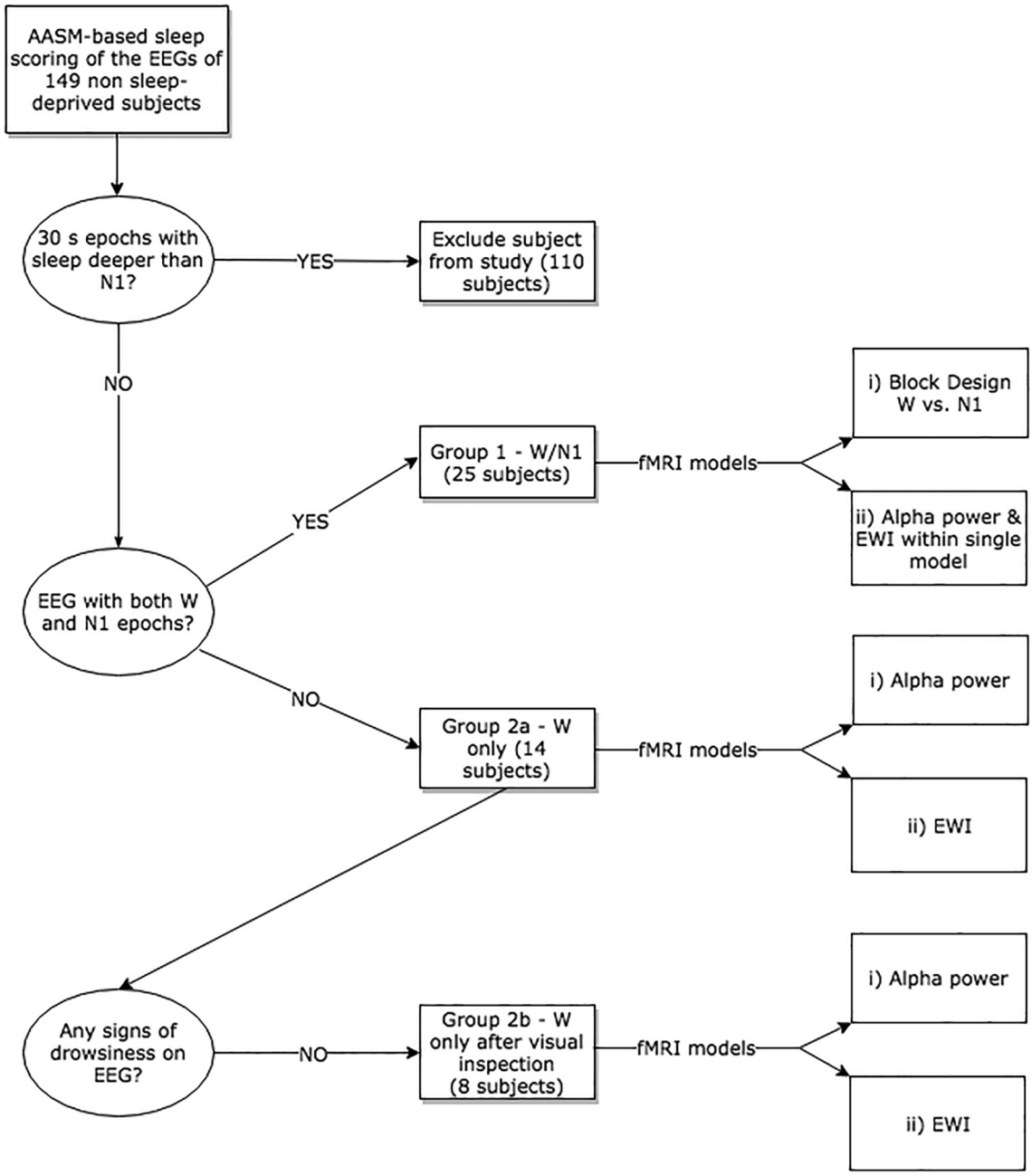

Fig. 1. Flow-chart illustrating the selection process of subjects resulting in formation of groups based on visual EEG inspection. AASM = American Academy of Sleep Medicine. EEG = Electroencephalogram. fMRI = functional Magnetic Resonance Imaging. EWI = EEG Wakefulness Index.

To summarize the frequency content across all EEG channels, we first performed a temporal principal component analysis (temporal PCA) of each multi-channel EEG data set and subsequently analysed the first component, i.e. the component explaining the maximum amount of data variance. We will term this one-dimensional time series PCA-1.

We then computed a time-frequency spectrogram of the PCA-1 time series using a continuous wavelet transform (CWT) based on a Morlet mother wavelet (parameter $\sigma_0 = 6$, Torrence and Compo, 1998). The CWT spectrograms define a frequency spectrum at each single time point, taking into account the frequency content in a neighbourhood of that point as defined by the width of the wavelet. As the hypnogram assigns each time point to either W or N1, separate W and N1 spectra are obtained by averaging the CWT spectrograms over the corresponding time segments.

We thus obtained 25 spectra for the W and N1 vigilance states, respectively.

2.6. Construction of the block design

We hypothesised that the BOLD patterns previously (Goldman et al., 2002; Moosmann et al, 2003; Laufs et al., 2006) found to be negatively correlated with EEG alpha power featuring a parieto-occipital pattern were due to reduced wakefulness, i.e. light sleep. To test this hypothesis, we used a block design in Statistical Parametrical Mapping (SPM5, http://www.fil.ion.ucl.ac.uk/spm/) in which we compared differences in brain activity between wakefulness (W) and light sleep (N1) as determined by the AASM sleep scoring (AASM, 2007). Accounting the individual drift of our scanner (see the following paragraph), we set the high pass filter to 300 s.

2.7. MRI signal drift

Scanner imperfections and heating result in non-white noise ("drift") in the imaging data (Lund et al., 2006). The scanner drift is a result of an inaccuracy in the radio frequency, which is caused by vibration-induced heat dissipating to the main gradients. This drift induces an apparent translation of the brain in the direction of the y-axis (see Supplementary Fig. S2 for an example). We assessed the non-white noise of our particular setup, and checked whether realignment of our EPI images was effective in removing the spatial drift. To avoid such confound, commonly imaging studies apply a high pass filter to the data removing the low frequency drift. The default setting in SPM was once empirically determined on a Siemens Vision scanner and a large safety margin added resulting in a high-pass filter cut-off at 128 s. As our subjects of the W/N1 group sometimes remained in one sleep stage for longer than 128 s, a 128 s high pass filter would severely distort the block design and at least partially remove the signal of interest. Therefore, measuring the spontaneous BOLD signal change before and after image realignment served to identify for our setup a suitable high-pass filter significantly reducing the signal drift while preserving slow fluctuations. This facilitated the preservation and identification of signal changes induced by the switching between epochs of wakefulness and drowsiness (N1).

2.8. Construction of the EEG wakefulness index (EWI)

AASM rules (AASM, 2007) define sleep stages based on 30 s epochs. In order to non-visually detect fluctuations between W and N1 and with a higher temporal resolution than the 30 s epochs, we constructed a wakefulness measure (henceforth called EEG wakefulness index; EWI) that relied on both spectral and topographical instantaneous EEG information. The goal was to construct a ratio that carries the power of EEG components with a higher amplitude during wakefulness (W > N1) in the numerator, and to put those with higher power during drowsiness (N1 > W) in the denominator. The EEG components (frequencies and topography) were chosen according to the available literature on wake-sleep transitions. The ratio (EWI) was defined as:

$$r = \frac{p(\vartheta, F_{3,4}) + p(\alpha, O_{1,2}) + p(\sigma, O_{1,2}) + p(\beta, F_{3,4})}{p(\delta, F_{3,4}) + p(\vartheta, O_{1,2}) + p(\sigma, C_{3,4}) + p(\alpha, F_{3,4}) + p(\beta, F_{3,4})}$$

where p (ϑ, $F_{3,4}$), for example, denotes the instantaneous power in the theta frequency band (ϑ, 4–8 s^{-1}), averaged across the frontal EEG channels *F3* and *F4*. The other terms are interpreted accordingly. Using the analytical amplitude of the individual frequency bands, the term is evaluated at each time point. For better visibility, time dependence is not included in the equation.

The EEG frequency bands were defined as follows:

δ: 0.5/s–4/s
ϑ: 4/s–8/s
α: 8/s–12/s
σ: 12/s–15/s
β: 16/s–30/s

The individual terms are justified as follows: Tinguely et al. (2006) found respective maxima in frontal derivations for theta and beta, and in occipital derivations for alpha and sigma during wakefulness. We included occipital alpha as it is generally accepted as the indicator of quiet wakefulness (Rechtschaffen, 1968; De Gennaro et al., 2001; AASM, 2007). Regarding the denominator of the ratio, Broughton and Hasan (1995) found delta to have its maximum at frontal derivations during drowsiness and so did Tinguely and colleagues (2006). Theta power was described to be maximal at occipital derivations during drowsiness (Wright et al., 1995; Tinguely et al., 2006). Sigma power was observed to be maximal centrally shortly after sleep onset (Broughton and Hasan, 1995; De Gennaro et al., 2001; Tinguely et al., 2006). The so-called anteriorisation of alpha oscillations during the sleep-wake transition is an indicator of drowsiness (Davis et al., 1937; Hori, 1985; Wright et al., 1995; Broughton and Hasan, 1995; Cantero et al., 1999; De Gennaro et al., 2001 and Tinguely et al., 2006) and found entry into clinically widely used scoring manuals (Rechtschaffen, 1968; AASM, 2007). Beta power appears to be maximal at frontal derivations also during drowsiness (Tinguely et al., 2006). This is probably due to the appearance of sleep spindles with beta band oscillatory activity during drowsiness (Kubicki and Herrmann, 1996). Placing the term p (β, $F_{3,4}$) in both, the numerator and the denominator of the EEG wakefulness index, is reasonable as beta band oscillations have a different functional role in wakefulness and drowsiness, respectively.

Please refer to Fig. 2B for an exemplary time course of the EWI and the corresponding hypnogram of a single subject.

The power for each frequency band was computed using a zero-phase 6th order Butterworth band-pass filter and the amplitude of the filtered signal's Hilbert transform. Subsequently, we down-sampled the signals in order to obtain one data point per TR and convolved the resulting signal with the canonical hemodynamic response function (HRF) as provided by SPM.

2.9. Construction of the alpha power regressor

In the same way, we calculated the average occipital alpha band power as the mean amplitude of the two occipital EEG leads O1 and O2 and convolved it with the hemodynamic response function (Laufs et al., 2003a). Please refer to Fig. 2A for the time course of occipital alpha power and the corresponding hypnogram of a single subject.

2.10. Correlation of the EEG wakefulness index and occipital alpha power with the hypnograms

We correlated the EWI as well as occipital alpha power with each subject's hypnogram as defined by AASM criteria (Pearson correlation). We compared the different correlation coefficients by using an asymptotic Wilcoxon-Test.

2.11. Discrimination of the EWI and occipital alpha power between clinical sleep stages

In order to test the discriminatory power of the EEG wakefulness index with regard to wakefulness (W) and light sleep (N1) as defined by AASM-criteria, we performed a receiver operating characteristic analysis. For better comparison, we also performed the receiver operating characteristic analysis on occipital alpha power.

2.12. fMRI models

Data from Group 1 ("W/N1") was analysed in three different ways (Fig. 1):

(i) In order to determine differences in brain activity between wakefulness (W) and light sleep (N1), we constructed a block design as explained above.
(ii) In order to detect changes in brain activity during the transition between wakefulness and light sleep based on a change in occipital alpha power, we convolved the alpha power regressor with the HRF and included it in the model (see below). Furthermore, in order to detect signal fluctuations

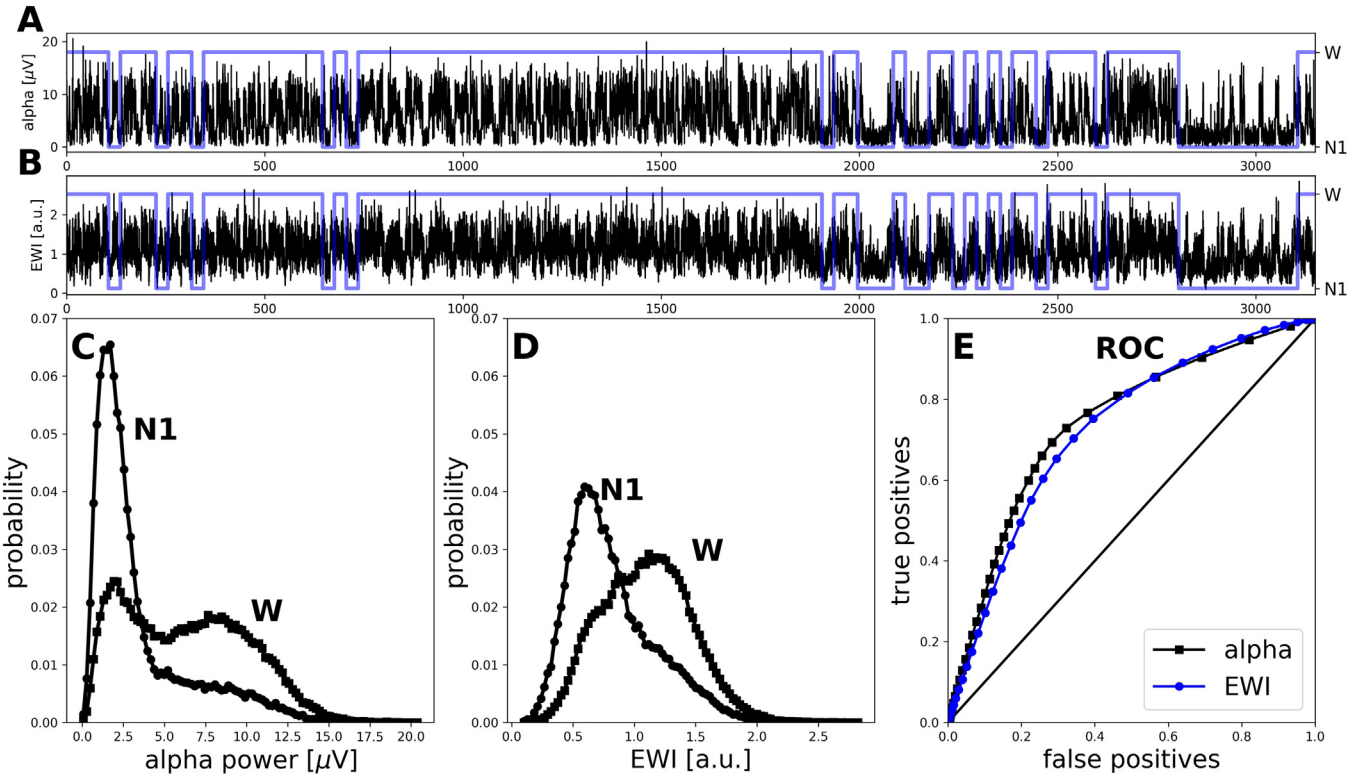

Fig. 2. Exemplary wake (W) and drowsiness (N1) analysis of a single subject. A: Alpha power expressed as the analytical amplitude of the alpha rhythm (8–12 Hz, black) and the corresponding hypnogram calculated from 30 s. data blocks according to standard AASM sleep scoring rules (light blue, upper value: awake, 'W', lower value: drowsiness, 'N1'). Longer W and N1 blocks contain short periods of fluctuating alpha power, indicating faster dynamics of W-N1 transitions than captured by the hypnogram. B: Time course of the EEG-derived wakefulness index (EWI, black) and the same hypnogram as in A. The EWI time course shows fluctuations similar, but not identical to the analytical alpha amplitude, and also contains up-down transitions which are faster than the hypnogram. C: Distribution of alpha power in AASM-defined wakefulness (W) and drowsiness/light sleep (N1) episodes. Alpha power values during AASM wakefulness yield a bimodal distribution due to the large scoring interval of 30 s, assigning short periods of low alpha, possibly indicating drowsiness, to the AASM wake state. D: Distributions of EWI values in AASM-defined wakefulness (W) and drowsiness/light sleep (N1) episodes. The unimodal distribution of EWI values during AASW-defined wakefulness suggests less N1-intrusions into the wake state when compared to the bimodal alpha power shown in C. E: Receiver operating characteristic (ROC) comparing the true and false positive detection rates of alpha power and EWI-based W/N1 assignments using the AASM-based hypnogram as the reference. ROC curves are constructed using n = 50 thresholds spanning the range of values of the underlying statistic (alpha power or EWI). We observe that the EWI classifies W and N1 with similar efficiency as the alpha power criterion. However, alpha power shows a slightly better performance (upper ROC) as expected by the purely alpha power based definition of W and N1 by AASM. The chance level is indicated by the diagonal line.

in brain activity between wakefulness and light sleep at a time scale shorter than 30 s, we convolved the EWI with the HRF and included it in the same general linear model (GLM) alongside the alpha power regressor in order to detect activations that are mutually exclusive to the alpha power and the EWI.

Data from Group 2a ("W only") was analysed in two different ways:

(i) In order to determine differences in brain activity corresponding to alpha power fluctuations, we convolved the alpha power regressor with the HRF and used it as the regressor of interest in a GLM.
(ii) In order to detect changes in brain activity based on EEG signal fluctuations usually found during the transition between wakefulness and drowsiness, we convolved the EEG wakefulness index with the HRF to form a regressor of interest in a GLM.

Data from Group 2b ("W only after visual inspection") was analysed as follows:

(i) In order to detect changes in brain activity in those subjects who did not display any signs of drowsiness, we convolved the alpha power regressor with the HRF and used it as the regressor of interest in a GLM.
(ii) In order to detect changes in brain activity based on EEG signal fluctuations usually found during the transition between wakefulness and drowsiness, we convolved the EWI with the HRF to form a regressor of interest in a GLM.

Cardiac, respiratory (as estimated by the RETROICOR method (Glover et al., 2000)) and motion-induced noise (with an autoregressive moving average model described by Friston et al, 1996) were modelled as confounds in all fMRI models (Jahnke et al., 2012).

2.13. fMRI group analysis

For all designs, we performed second level random effects group analyses by means of a one sample t-test of the contrast images corresponding to the respective contrasts of interest at the first level: the block regressors (convolved with the canonical hemodynamic response function (HRF) and its first temporal derivative (dHRF/dt)), the EEG wakefulness index (HRF-convolved) and the alpha power regressor (HRF-convolved), respectively.

2.14. Random effects group analysis

We performed second level random effects group analyses by means of two sample t-tests on the contrast images related to

HRF-convolved occipital alpha power changes for Group 1 (W/N1, 25 subjects) versus Group 2a (W only according to AASM rules, 14 subjects) and 2b (W only after strict visual inspection [exclusion of even brief N1-like epochs], 8 subjects), respectively.

3. Results

3.1. Power spectral densities for Group 1 (W/N1)

We analysed all 25 subjects in Group 1 whose hypnograms featured exclusively wakefulness (W) and light sleep (N1) with regard to the power spectral densities. We thus obtained 25 spectra for the W and N1 vigilance states, respectively. All individual spectra are shown in Supplementary Fig. S1. We observed that wakefulness (Supplementary Fig. S1A) was characterized by a dominant peak in the alpha frequency band, while light sleep (Supplementary Fig. S1B) still contained similar amounts of alpha and theta activity. Both observations are in accordance with AASM sleep scoring rules and with the EEG sleep physiology literature.

3.2. MRI signal drift

We analysed different sleep stages by means of a block design. In order to validate this analysis approach, we had to consider the effect of a spatial drift, which can be observed in any prolonged BOLD-fMRI recording: A problem for task-free fMRI studies is that MRI gradient heating may add coloured noise drifts to the recorded data, especially if the block lengths are tens of seconds long (Lund et al., 2006). For this reason, a high-pass filter is usually set in functional imaging software packages – in SPM it is empirically set to 128 s. This, however, imposes a problem for our design with long blocks resulting from subjects who remained in one sleep stage for more than 128 s. Investigation of a random sub-sample of 23 subjects revealed that indeed realignment reduced such scanner drift-induced effects (see Supplementary Figs. S3 and S4 for an example): On average, in this subpopulation, the realignment procedure extended the time until the BOLD signal change had drifted beyond one standard deviation. The time for this spatial drift was 187 s (+/− 9 s standard error of the mean) before (pre-alignment) and 463 s (+/− 28 s SEM) after realignment (post-realignment mean). Therefore, we increased the high pass filter setting to 300 s facilitating a valid analysis of blocks with lengths up to 300 s while still being protected against the technical drift.

3.3. Correlation of the EWI and occipital alpha power with the hypnograms

We correlated (Pearson's R) the EWI as well as alpha power with the hypnogram of each subject as defined by AASM criteria. The mean Pearson correlation of the EWI with the hypnogram was 0.18 (median 0.13; Supplementary Fig. S5A). The mean correlation coefficient of occipital alpha power with the hypnogram was 0.18 (median 0.11; Supplementary Fig. S5B). The Wilcoxon test of the correlation coefficients of the EWI and occipital alpha power did not yield significant results ($z = -1.4$, $p = 0.17$).

3.4. Discrimination of the EWI and alpha power between sleep stages

Testing the ability of the EWI to discriminate between the clinical sleep stages W and N1, we performed a receiver operating characteristic analysis. Fig. 2E offers a good example of a single subject. While an uninformed classifier has a mean area under the curve (AUC; the diagonal in the example of Fig. 2E) of 0.5, the calculated mean AUC of the EWI was 0.66 (median 0.69; Supplementary Fig. S6A). The mean AUC of occipital alpha power was 0.69 (median 0.70; Supplementary Fig. S6B). The paired t-test of the AUC of the EWI and occipital alpha power yielded a t value of 1.9 with $p = 0.065$. Fig. 2C and 2D show the distribution of alpha power and EWI values, respectively, in wakefulness (W) and light sleep (N1) of a single subject.

3.5. Group 1: subjects exhibiting wakefulness and N1 sleep

(i) Block design wakefulness vs. N1 sleep

Using a block design, we determined the differences in BOLD activation patterns between the AASM-defined states of wakefulness (W) and light sleep (N1). We analysed a group of subjects who presented epochs of W and N1 during fMRI scanning. We did not find any significant signal changes at a threshold of $p < 0.05$, family-wise-error-corrected. Exploring the data at a more lenient threshold ($p < 0.001$, uncorrected), in light sleep (N1, "drowsiness"), the occipital, parietal and frontal cortices exhibited a BOLD signal increase compared to wakefulness (W, $p < 0.001$, uncorrected; Fig. 3A; Table 1), whereas the thalamus, posterior and anterior cingulate gyri showed higher activity in wakefulness than in light sleep (N1, $p < 0.001$, uncorrected; Fig. 3B; Table 2).

(ii) Alpha power regression and the EEG wakefulness index in a single model

The expression of occipital alpha waves is an important criterion of the AASM-based sleep classification procedure. We hence pursued an analysis approach reflecting this fact. We convolved the occipital alpha power time series with the canonical hemodynamic response function provided by SPM. Additionally, as a third characterization of wakefulness versus drowsiness, we based one analysis on the combination of different EEG power values from different channels, what we call the EEG wakefulness index (EWI). We put both the alpha power and the EEG wakefulness index into a single model for Group 1 (subjects exhibiting W and N1) in order to detect activations specific to each one of the regressors and explored the data at the previous uncorrected threshold. High alpha power values were correlated with an activation of the thalamus, putamen, lingual gyrus and superior temporal gyrus ($p < 0.001$, uncorrected; Fig. 4A; Table 3) and high values of the EEG wakefulness index with an activation of the anterior cingulate cortex ($p < 0.001$, uncorrected; Fig. 4B; Table 4). Inversely, low values of the EEG wakefulness index revealed a hippocampal activation surviving a multiple comparison correction at $p < 0.05$ (family-wise error, Fig. 5; Table 5) whereas low alpha power did not yield any activations even at a threshold of $p < 0.001$, uncorrected (not shown). Please note that the family-wise error correction exclusively refers to the number of voxels.

3.6. Group 2a (W-only, AASM)

(i) Alpha power regression

We also performed a regression analysis using the alpha power in those subjects who remained awake (according to AASM rules) throughout the experiment. We did not find any BOLD signal changes associated with the alpha power at the previous threshold ($p < 0.001$, uncorrected; not shown).

(ii) 4 EEG wakefulness index

Looking for brain activity changes related to the EEG wakefulness index in a separate analysis in the awake (according to AASM rules) subject cohort, we did not obtain any significant results at the previous threshold ($p < 0.001$, uncorrected; not shown).

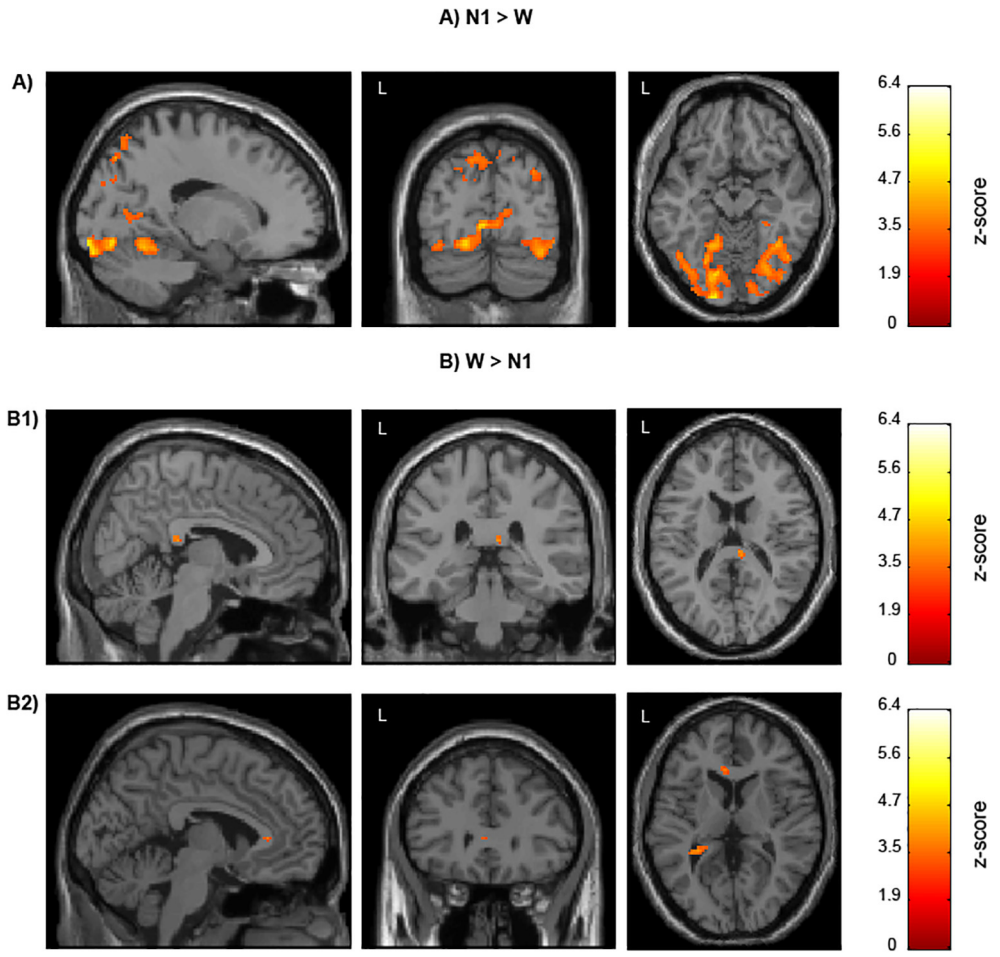

Fig. 3. BOLD signal changes correlated with drowsiness (N1) t-contrasted against wakefulness (W) and vice-versa displayed as color-coded z-values on a T1 MNI template brain ($p < 0.001$, uncorrected; voxel threshold 100 and 10 respectively; planes intersect at [−16; −80; −14] in panel A; at [6; −32; 16] in panel B1 and at [−4; 29; 6] in panel B2). Sleep stages N1 and W defined by AASM-criteria. This analysis (Group 1; W/N1) included 25 subjects. Refer to Tables 1 and 2 respectively for more details.

Table 1
Talairach peak coordinates, t- and z-scores of cluster maxima, cluster sizes and anatomical structures for BOLD signal changes correlated with drowsiness (N1) t-contrasted against wakefulness (W); $p < 0.001$, uncorrected; only cluster sizes larger than 100 voxels are listed. Refer to Fig. 3A for a visualisation.

Group 1, i; N1 > W							
Cluster maximum at			t	Z-score of cluster maxima	Number of voxels in cluster	Side	Region
X	Y	Z					
−18	−93	−7	7.19	5.20	2044	L	Inferior occipital gyrus
−30	−56	54	7.19	5.20	1195	L	Superior parietal lobule
31	−39	−13	6.74	5.00	819	R	Fusiform gyrus
27	−53	42	5.81	4.55	139	R	Superior parietal lobule
−32	−85	29	5.27	4.26	109	L	Superior occipital gyrus
−45	18	36	4.69	3.91	135	L	Precentral gyrus
−24	−65	26	4.55	3.83	120	L	Precuneus

Table 2
Talairach peak coordinates, t- and z-scores of cluster maxima, cluster sizes and anatomical structures for BOLD signal changes correlated with wakefulness (W) t-contrasted against drowsiness (N1); $p < 0.001$, uncorrected; only cluster sizes larger than 10 voxels are listed. WM = white matter; CSF = cerebrospinal fluid. Refer to Fig. 3B for a visualisation.

Group 1, i; W > N1							
Cluster maximum at			t	Z-score of cluster maxima	Voxels	Side	Region
X	Y	Z					
−19	−19	25	5.63	4.45	50	L	Caudate
25	5	27	5.13	4.17	30	R	WM
−23	−45	12	4.86	4.01	91	L	CSF
6	−31	17	4.72	3.93	18	R	Thalamus
−4	29	6	4.25	3.64	10	L	Anterior cingulate

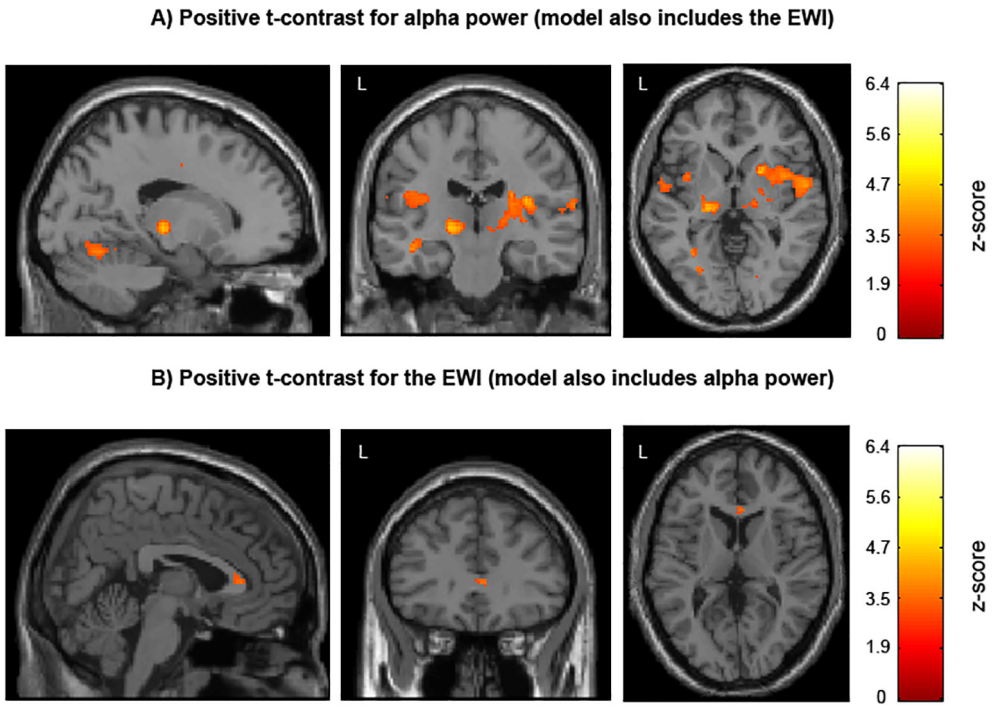

Fig. 4. BOLD signal changes positively correlated with occipital alpha power (A) and the EEG wakefulness index (B), respectively (in a single model including both regressors), displayed as color-coded z-values on a T1 MNI template brain (A: $p < 0.001$, uncorrected; voxel threshold 150; planes intersect at [−16; −20; 0]; B: $p < 0.001$, uncorrected; voxel threshold 10; planes intersect at [4; 32; 6]). This analysis (Group 1; W/N1) included 25 subjects. Refer to Tables 3 and 4 respectively for more details.

Table 3
Talairach peak coordinates, t- and z-scores of cluster maxima, cluster sizes and anatomical structures for BOLD signal changes correlated with high alpha power in a model including also the EEG wakefulness index; $p < 0.001$, uncorrected; only cluster sizes larger than 150 voxels are listed. Refer to Fig. 4A for a visualisation.

Group 1, ii; positive t-contrast for alpha power (model with EEG wakefulness index included as additional regressor)							
Cluster maximum at			t	Z-score of cluster maxima	Voxels	Side	Region
X	Y	Z					
25	7	8	6.91	5.16	2849	R	Putamen
−31	−55	2	6.89	5.15	2016	L	Lingual Gyrus
−15	−21	3	5.63	4.51	156	L	Thalamus
−40	−36	10	5.16	4.25	1664	L	Superior temporal gyrus
−9	7	39	5.05	4.18	658	L	Cingulate gyrus
45	−10	36	4.30	3.70	150	R	Precentral gyrus

Table 4
Talairach peak coordinates, t- and z-scores of cluster maxima, cluster sizes and anatomical structures for BOLD signal changes correlated with high values of the EEG wakefulness index in a model including also alpha power as a regressor; $p < 0.001$, uncorrected; only cluster sizes larger than 10 voxels are listed. Refer to Fig. 4B for a visualisation.

Group 1, ii; positive t-contrast for the EEG wakefulness index (model with alpha power included as additional regressor)							
Cluster maximum at			t	Z-score of cluster maxima	Voxels	Side	Region
X	Y	Z					
3	29	6	4.10	3.57	46	R	Anterior cingulate

3.7. Group 2b ("W only, strict visual inspection")

(i) Alpha power regression

We performed another regression analysis on a subgroup of Group 2a (W only after strict visual inspection). From the group of subjects exhibiting wakefulness only – according to AASM criteria (Group 2a), an EEG expert excluded any subject exhibiting even very brief episodes of drowsiness (e.g. drops in alpha activity, increased lower frequency power) even if those did not fulfil the formal and 30 s epoch-based AASM N1 scoring criteria. The remaining subjects who exhibited hardly any signs of drowsiness were re-analysed using posterior alpha power as a regressor. Again, we did not find any significant BOLD signal changes at the previously used uncorrected threshold level ($p < 0.001$; uncorrected; not shown).

(ii) EEG wakefulness index

Looking for brain activity changes related to the EEG wakefulness index in a separate analysis in the strictly awake (according to an EEG expert; Group 2b) subject cohort, we did not find any significant result at the previous threshold ($p < 0.001$, uncorrected; not shown).

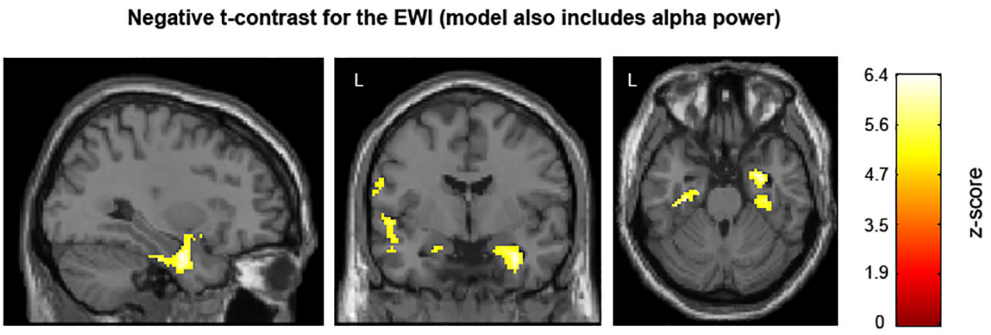

Fig. 5. BOLD signal changes negatively correlated with the EEG wakefulness index – indicating reduced wakefulness – (in a model including also alpha power as a regressor) displayed as color-coded z-values on a T1 MNI template brain ($p < 0.05$, FWE-corrected; voxel threshold 100; planes intersect at [32; −4; −26]). This analysis (Group 1; W/N1) included 25 subjects. Refer to Table 5 for more details. (For interpretation of the references to colour in this figure legend, the reader is referred to the web version of this article.)

Table 5
Talairach peak coordinates, t- and z-scores of cluster maxima, cluster sizes and anatomical structures for BOLD signal changes correlated with low values of the EEG wakefulness index in a model including also alpha power as a regressor; $p < 0.05$, FWE-corrected; only cluster sizes larger than 100 voxels are listed. Refer to Fig. 5 for a visualisation.

Group 1, ii; negative t-contrast for the EEG wakefulness index (model with alpha power included as additional regressor)							
Cluster maximum at			t	Z-score of cluster maxima	Voxels	Side	Region
X	Y	Z					
19	−3	−13	9.65	6.24	319	R	Parahippocampal gyrus
−30	−22	−19	8.92	5.99	116	L	Parahippocampal gyrus
−43	−16	−6	8.39	5.79	209	L	Insula
−57	−6	22	7.50	5.43	102	L	Precentral gyrus

3.8. Random effects group analysis

We performed a second level random effects group analysis by means of a two sample t-test comparing occipital alpha power related BOLD signal changes between Group 1 (W/N1) and Group 2a (W only according to AASM) and Group 2b (pure W without N1-like epochs confirmed by visual inspection), respectively. The t-test comparing the groups both containing brief N1 or N1-like epochs, i.e. Group 1 and Group 2a, did not yield any results at $p < 0.001$ (uncorrected; not shown). Yet, in the comparison contrasting Group 1 against Group 2b, we found activity changes in the thalamus and the cerebellum ($p < 0.001$; uncorrected; Supplementary Fig. S7 and Supplementary Table S1) suggesting differential alpha power-associated activity in the aforementioned regions when contrasting a group of subjects including N1 epochs – in addition to W – with a group devoid any N1-like epochs. We did not find any alpha power-associated signal changes for the opposite comparison, i.e. Group 2b vs. Group 1 ($p < 0.001$, uncorrected; not shown).

4. Discussion

In the present study, we sought to identify brain regions changing their activity depending on EEG spectral characteristics and the state of vigilance, i.e. wakefulness (W) and light sleep (N1). In particular, we were interested to see whether any such changes are a net effect of the gross state or can be traced based on continuous measures of neuronal activity derived from surface EEG. Accordingly, we examined two groups of subjects: subjects exhibiting two states during the experiment, i.e. wakefulness and N1 sleep (Group 1) and subjects remaining exclusively in the awake state (Group 2). For Group 1, we assessed (I) state-associated BOLD signal changes by means of a block design (N1 versus W). Further, we calculated BOLD signal changes correlated with fluctuations in posterior surface EEG-derived alpha power as well as a combination of EEG features (a ratio of linear combinations of different frequency band powers, including topographic information) thought to gradually change with increasing or decreasing wakefulness ("EEG wakefulness index", EWI). We combined analysis of alpha power and the EEG wakefulness index within a signal model (II) in order to detect differential effects of alpha power fluctuations and the brain state as indicated by the EWI.

Results were significant at a conservative threshold with family-wise error (FWE) correction for the analysis, which was based on a combination of EEG-derived band power values, i.e. the EEG wakefulness index. This revealed bilateral hippocampal BOLD signal increases with increasing drowsiness when modelled alongside the alpha regressor (II). Briefly, the continuous measures appeared to detect BOLD signal changes more sensitively than the state-dependent block designs.

We report additional results, which in isolation did not meet the stringent statistical threshold of FWE-corrected $p < 0.05$ mentioned above. Nevertheless, we consider their presentation justified because different analyses resulted in concordant results. This reduces the likelihood of them occurring by mere chance. We summarise these in the following three paragraphs.

More active during drowsiness (N1) than during wakefulness in terms of associated BOLD signal changes were parieto-occipital regions in the block designs comparing W and N1 (I) affirming our previous hypothesis (Laufs et al., 2006).

Across three analyses, we detected increased thalamic activity for measures indicating or being more associated with wakefulness than drowsiness: 1. The block design W > N1 (I); 2. high alpha power (II) in the group of subjects with both W and N1 in their sleep profile (Group 1); 3. in the random effects group analysis comparing Group 1 (W and N1) with group 2b (W only without N1-like epochs ascertained by strict visual inspection).

In two analyses, the BOLD signal increases occurred in the anterior cingulate cortex with increased wakefulness as assessed by (1) the block model (W > N1, I) and (2) the EEG wakefulness index (II).

Not in any of the wake-only cohorts (Group 2) did we reveal significant BOLD signal changes in the anterior cingulate cortex.

4.1. Evaluation of the EEG wakefulness index

We evaluated the EEG wakefulness index in terms of (a) its correlation with each subject's hypnogram as defined by AASM criteria and (b) its ability to discriminate the sleep stages W and N1. The EWI and occipital alpha power effectively had an identical degree of correlation with the hypnogram. The discriminatory power of the EWI with regard to wakefulness (W) and light sleep (N1) was equal to that of the spectral alpha data. These sleep stages are based on clinical EEG criteria which are independent of the EWI. We argue that the amplitude of each frequency band, on which the EWI is based, contributes to its discriminatory power. This is in line with the AASM-based clinical sleep scoring, in which light sleep is defined as "low amplitude, mixed frequency activity" among other criteria (AASM, 2007).

4.2. fMRI-correlates of EEG-alpha-rhythm are vigilance dependent

We used several measures reflecting wakefulness and drowsiness in different manners to shed light on the observation that the previous literature reported at least two different activation maps when negatively correlating alpha power with the BOLD time course. One is a pattern with occipital emphasis (Goldman et al., 2002; Laufs et al., 2003a; Moosmann et al., 2003), the other one that of a bilateral frontal-parietal pattern (Laufs et al., 2006). Spectral analysis of EEG recordings revealed that the "occipital map" also correlated positively with low beta and high theta band power, whereas in subjects exhibiting the frontal-parietal map the relationship with these frequency bands was inverted. Our group hence had suggested (Laufs et al., 2006) that these maps might reflect different brain states dependent on whether subjects were awake only or undulated between W and N1. Since an increase in theta power with concurrent decrease in alpha power are indicators of drowsiness (AASM, 2007), we had hypothesized that the occipital pattern was linked to a state of decreased vigilance. Support for our hypothesis came from a later study, which used an EEG-vigilance classifier (Olbrich et al., 2009). The frontal-parietal pattern matches a functional attentional system. In our present study, we were able to identify the occipital map only in the block design contrasting sleep stage N1 against W. This is in line with the interpretation that this map does indeed reflect the brain state of decreased vigilance rather than a directly awake alpha power-bound set of brain regions. Anticipating the revelation of the frontal-parietal attentional BOLD pattern negatively correlated with the alpha power in the W-only group we could not reproduce this pattern. A possible explanation is that episodes of clear sleep are required to be intermixed with wakefulness in order that frontal-parietal brain regions intermittently "deactivate" and hence this pattern can be detected. This can explain why in subjects, whose EEG recordings fulfilled W criteria (according to AASM rules) only, not any of our models revealed this pattern. In line with the previous observation, when we formed a subgroup of eight subjects who exhibited hardly any signs of drowsiness in their EEG recordings at all, we did not detect any related frontal-parietal, nor any other BOLD signal pattern, either. This suggests that "pure" wakefulness is not associated with large enough fluctuations in the frontal-parietal attentional system for them to be reflected in posterior alpha oscillations – and related fMRI signal changes. This is in contrast to when continuous, true wakefulness (high alpha power) and sleep (low alpha power) are mixed: when comparing Group 1 (W/N1 according to AASM criteria), which includes N1 epochs, with pure wakefulness, i.e. not "contaminated" by brief N1-like epochs, we detected thalamic signal changes. This was so despite the fact that power in the latter comparison (24 subjects vs. 8 subjects) was less (Friston et al., 1999) than in the comparison of the subjects exhibiting both W and N1 (Group 1) with those exhibiting W only according to AASM – not prohibiting N1-like epochs of less than 30 s (24 vs. 14 subjects).

Clinically established visual scoring rules allow N1 features to occur during up to 50 % of the time in epochs classified as wakefulness. Such rules are consequently unsuitable to isolate states of "pure" wakefulness not "contaminated" by drowsiness – and vice-versa. For clinical purposes, the trade-off between feasibility and clinical necessity on the one hand and sensitivity on the other appears well struck. The lack of N1-sensitivity of such a method, however, might explain the lack of significant fMRI results in some of our analyses when W and N1 features were intermixed in the fMRI data but not reflected in the corresponding model. Yet, for functional imaging experiments during rest, fluctuations in wakefulness are relevant because they are associated with BOLD-fMRI signal changes and affect the results, which require special consideration in interpretation (Tagliazucchi and Laufs, 2014).

4.3. Activation of the thalamus and the anterior cingulate cortex during wakefulness

Our model based on the alpha power regressor (II) yielded BOLD signal increases with increased alpha power within the thalamus. We obtained similar results when contrasting wakefulness against N1 sleep in the block design (I). However, we could reproduce these results in Group 1 (W/N1) but not in Group 2 (W only). This suggests that during relaxed wakefulness without relevant intrusions of drowsiness and with regard to the hemodynamic measures obtained in this study, there is a rather constant activation of these regions, which renders them undetectable for our models. This could explain why neither the model based on the fluctuations of alpha power nor the model based on the EEG wakefulness index detected a significant change in activation within those regions. Thus, activation of the thalamus seems dependent on the state of vigilance (wakefulness versus sleep). This can be seen in analogy to the described tonic firing mode of thalamic neurons during wakefulness versus the more burst-like activity during deeper sleep (Weyand et al., 2001) and complements the reduction of thalamic functional connectivity during early sleep and with decreasing occipital alpha power compared to wakefulness (Scheeringa et al., 2012; Tagliazucchi et al., 2012; Chang et al., 2013).

Analysis of the slight fluctuations between wakefulness and light sleep by means of EEG power bands may not be sensitive enough for the detection of thalamic mode switches (tonic vs. phasic) as this analysis included only those subjects in wakefulness and light sleep but not any individuals reaching deeper sleep stages (N2, N3). In our Group 2 (W only), the variance of alpha power might be too small to yield a significant BOLD signal change in the thalamus. This hypothesis is supported by the fact that – when comparing alpha power-associated signal changes in Group 1 with those of Groups 2a and 2b, respectively, we found a bilateral thalamic activation for Group 1 only in the comparison with Group 2b ("pure" W). Comparison of Group 1 (W/N1) to Group 2a (W only by AASM criteria – not excluding brief N1-like epochs) did not yield any thalamic activity changes. This might be due to similar alpha power variance across these two groups. By AASM definition, the sleep stage W may feature mixed low frequency activity up to 50 % of each 30 s epoch. When the subjects featuring those frequencies (Group 2b) are excluded from the analysis, thalamic activation is found for Group 1 compared to Group 2b. This, again, highlights the limits of the AASM criteria when applied in non-clinical settings.

Alternatively – assuming that alpha oscillations reflect thalamic activity (Becker et al., 2015; Chen et al., 2015) – their presence would imply that thalamic activity remains tonic. When contrasting wakefulness against light sleep in a block design (I), however, we found a significant activation in both the anterior cingulate cortex and the thalamus. This result is in line with models of alpha generation in thalamo-cortical circuits (Lopes da Silva et al., 1974; Valdes et al., 1999) and was found in other studies using simultaneous EEG-fMRI recordings, too (Goldman et al., 2002; Feige et al., 2005; Goncalves et al., 2006; Difrancesco et al., 2008). Our own group found a reduction in thalamic functional connectivity in sleep compared to wakefulness and linked to alpha power (Tagliazucchi et al., 2012). There is also ample – including clinical – evidence for the thalamus' role in sustaining wakefulness (Lopez-Serna et al., 2009). However, different reference electrode positions across the mentioned studies hinder the comparison of these EEG analyses but vigilance-dependent global alpha power changes might be less affected by the exact montage.

Studies reported the thalamus and the anterior cingulate cortex (ACC) as part of a network responsible for maintenance of non-selective alertness (Sadaghiani et al., 2010). We analysed both the alpha power and the EEG wakefulness index within a single model (II) in order to detect activations mutually exclusive to each regressor. Interestingly, high alpha power identified an activation of the thalamus, whereas high values of the EEG wakefulness index revealed the activation of the ACC. The former lends support to the existence of a specific link between alpha oscillations and thalamic (BOLD) activity (Becker et al., 2015; Chen et al., 2015). The latter implies that the EEG wakefulness index co-varies with a more general process involving the anterior cingulate cortex. Furthermore, while being co-activated as part of a so-called cingulo-insular-thalamic network as hypothesised by Sadaghiani (Sadaghiani et al., 2010), there is also research linking ACC and thalamus to functionally different networks, the salience network and the executive-control network (Seeley et al., 2007) - which could be reflected by our results, too. However, said study features a higher spatial resolution than our present study, and Sadaghiani and colleagues were able to distinguish between anterior thalamus, which is part of the salience network, and dorsomedial thalamus as part of the executive-control network. Further studies with a higher spatial resolution should shed more light onto these aspects.

4.4. Detection of hippocampal and ACC BOLD signal changes by use of the EEG wakefulness index

We constructed the EEG wakefulness index (II, higher values indexing higher degrees of wakefulness) in order to take advantage of both spectral and topographical properties of the EEG during the transition from wakefulness to light sleep. Both the positive and negative correlation of the regressor with the BOLD time series led to significant, functionally coherent results: The ACC correlated positively, the hippocampus negatively with this wakefulness index.

The finding of an increase in hippocampal activity during light sleep compared to wakefulness is a novel finding which we did not see reported in any similar study so far, even though it resulted from exploration. This includes analyses by means of alpha power as a marker of drowsiness (Goldman et al., 2002; Moosmann et al., 2003; Laufs et al., 2003a,b, Laufs et al., 2006) or by using a sleep stage classification (Olbrich et al., 2009) and our own block design analysis presented here. One study (Picchioni et al., 2008) compared early and late sleep stage 1 (Rechtschaffen, 1968) and found an increase in hippocampal activation in late sleep stage 1 compared to early stage 1 sleep.

One possible explanation for the observed hippocampal activation common during light sleep is its role in memory consolidation during sleep. Although in this resting state study we did not present any material aimed at homogenous encoding, any "various" material to which the subjects were exposed during the day should stimulate some sort of memory encoding and consolidation. Sleep is considered the period and state in which newly acquired information is consolidated in memory (Diekelmann and Born, 2010). In declarative memory consolidation, the hippocampal formation functions as a location for temporary storage from which memory is redistributed to a long-term storage, in this case the neocortex (Frankland and Bontempi, 2005). This process is thought to happen during slow wave rather than REM sleep (Barrett and Ekstrand, 1972; Plihal and Born, 1997). REM sleep is understood to favour procedural memory consolidation (Maquet, 2001) over declarative memory consolidation. A study by Lahl et al. (2008) showed that – although the longer sleep, the better memory retention – a nap as short as six minutes can facilitate memory improvement. Lahl did not study subjects during slow wave sleep, instead they were in sleep stage 2 (Rechtschaffen, 1968) for less than one third of their total sleep time only. Thus, subjects predominantly exhibited sleep stage 1 (Rechtschaffen, 1968) which conforms to N1 in our present study (AASM, 2007). Though not explicitly studied but already discussed by Lahl and colleagues, one can assume an involvement of the hippocampus in declarative memory consolidation during the subjects' short naps because of its mentioned role in fast temporary storage of memory traces during sleep. Furthermore, due to the comparable nature of sleep stages analysed in Lahl's and our study, respectively, the activation of the hippocampus in our study could hint to a memory consolidation occurring also in light sleep. Admittedly, our subjects did not perform any learning tasks for which we could have tested after the fMRI scan. Nevertheless, as the scans were performed in the evening and therefore close to the subjects' usual sleeping times, it is likely that indeed memory consolidation took place in our subjects involving the hippocampus (an explicit learning task during the day is not required for the process of memory consolidation to occur).

5. Conclusion

In conclusion, we present evidence that fMRI activation patterns related to EEG alpha oscillations reflect different brain states associated with different levels of wakefulness. We were able to characterize the states more finely grained when we included in our analyses EEG frequency information both above and below the alpha band. Our findings suggest that typical "alpha fMRI studies" during rest detect thalamic BOLD signal changes if state switches between wakefulness and drowsiness occur and if these are modelled accurately. We found an increase in BOLD activity in parieto-occipital regions to be bound to indices of light sleep suggesting that earlier work linking this pattern to alpha-desynchronization studied subjects exhibiting drowsiness. Exploiting EEG features with high temporal resolution, we revealed hippocampal activity changes during light sleep compared to wakefulness supporting the idea that memory encoding might already take place in that early state of sleep. Finally, the clinician's eye can track changes in alpha oscillations related to thalamic activity changes to which clinically established sleep scoring rules are insensitive.

Acknowledgments

This work was funded by the Bundesministerium für Bildung und Forschung (grant 01 EV 0703) and LOEWE Neuronale Koordination Forschungsschwerpunkt Frankfurt (NeFF). We thank Verena Brodbeck for visually re-scoring our awake subjects (Group 2). This study was part of a set of experiments designed as a simultaneous

EEG-fMRI study on sleep physiology. Previous data of the same series, which has been published, includes Jahnke et al., 2012, Tagliazucchi et al., 2012 and Tagliazucchi and Laufs, 2014.

Declaration of Competing Interest

None.

Appendix A. Supplementary material

Supplementary data to this article can be found online at https://doi.org/10.1016/j.clinph.2019.04.715.

References

Allen PJ, Polizzi G, Krakow K, Fish DR, Lemieux L. Identification of EEG events in the MR scanner: the problem of pulse artifact and a method for its subtraction. NeuroImage 1998;8(3):229–39.

American Academy of Sleep Medicine. The AASM manual for the scoring of sleep and associated events: rules, terminology and technical specifications. Westchester, IL: American Academy of Sleep Medicine; 2007.

Barrett TR, Ekstrand BR. Effect of sleep on memory. 3. Controlling for time-of-day effects. J Exp Psychol 1972;96(2):321–7.

Becker R, Knock S, Ritter P, Jirsa V. Relating alpha power and phase to population firing and hemodynamic activity using a thalamo-cortical neural mass model. PLoS Comput Biol 2015;11(9).

Berger H. Über das Elektrenkephalogramm des Menschen. Archiv f Psychiatrie 1929;87(1):527–70.

Broughton R, Hasan J. Quantitative topographic electroencephalographic mapping during drowsiness and sleep onset. J Clin Neurophysiol 1995;12(4):372–86.

Cantero JL, Atienza M, Gómez CM, Salas RM. Spectral structure and brain mapping of human alpha activities in different arousal states. Neuropsychobiology 1999;39(2):110–6.

Chang C, Liu Z, Chen MC, Liu X, Duyn JH. EEG correlates of time-varying BOLD functional connectivity. NeuroImage 2013;72:227–36.

Chen Z, Wimmer RD, Wilson MA, Halassa MM. Thalamic circuit mechanisms link sensory processing in sleep and attention. Front Neural Circ 2015;9:83.

Davis H, Davis PA, Loomis AL, Harvey EN, Hobart G. Human brain potentials during the onset of sleep. J Neurophysiol 1937;1:24–37.

Diekelmann S, Born J. The memory function of sleep. Nat Rev Neurosci 2010;11(2):114–26.

Difrancesco MW, Holland SK, Szaflarski JP. Simultaneous EEG/functional magnetic resonance imaging at 4 Tesla: correlates of brain activity to spontaneous alpha rhythm during relaxation. J Clin Neurophysiol 2008;25(5):255–64.

Feige B, Scheffler K, Esposito F, Di Salle F, Hennig J, Seifritz E. Cortical and subcortical correlates of electroencephalographic alpha rhythm modulation. J Neurophysiol 2005;93(5):2864–72.

Frankland PW, Bontempi B. The organization of recent and remote memories. Nat Rev Neurosci 2005;6(2):119–30.

Friston KJ, Williams S, Howard R, Frackowiak RSJ, Turner R. Movement-Related effects in fMRI time-series. Magn Reson Med 1996;35(3):346–55.

Friston KJ, Holmes AP, Worsley KJ. How many subjects constitute a study? Neuroimage 1999;10:1–5.

de Gennaro L, Ferrara M, Bertini M. The boundary between wakefulness and sleep: Quantitative electroencephalographic changes during the sleep onset period. Neuroscience 2001;107(1):1–11.

Glover GH, Li TQ, Ress D. Image-based method for retrospective correction of physiological motion effects in fMRI: RETROICOR. Magn Reson Med 2000;44(1):162–7.

Goldman RI, Stern JM, Engel J, Cohen MS. Simultaneous EEG and fMRI of the alpha rhythm. NeuroReport 2002;13(18):2487–92.

Goncalves SI, de Munck JC, Pouwels PJW, Schoonhoven R, Kuijer JPA, Maurits NM, et al. Correlating the alpha rhythm to BOLD using simultaneous EEG/fMRI: inter-subject variability. NeuroImage 2006;30(1):203–13.

Hori T. Spatiotemporal changes of EEG activity during waking-sleeping transition period. Int J Neurosci 1985;27:101–14.

Jahnke K, von Wegner F, Morzelewski A, Borisov S, Maischein M, Steinmetz H, et al. To wake or not to wake? The two-sided nature of the human K-complex. NeuroImage 2012;59(2):1631–8.

Jensen O, Mazaheri A. Shaping functional architecture by oscillatory alpha activity: gating by inhibition. Front Hum Neurosci 2010;4:186.

Johns MW. A new method for measuring daytime sleepiness: the Epworth sleepiness scale. Sleep 1991;14:540–5.

Kubicki S, Herrmann WM. The future of computer-assisted investigation of the polysomnogram: sleep microstructure. J Clin Neurophysiol 1996;13(4):285–94.

Lahl O, Wispel C, Willigens B, Pietrowsky R. An ultra short episode of sleep is sufficient to promote declarative memory performance. J Sleep Res 2008;17(1):3–10.

Laufs H, Holt JL, Elfont R, Krams M, Paul JS, Krakow K, Kleinschmidt A. Where the BOLD signal goes when alpha EEG leaves. NeuroImage 2006;31(4):1408–18.

Laufs H, Kleinschmidt A, Beyerle A, Eger E, Salek-Haddadi A, Preibisch C, et al. EEG-correlated fMRI of human alpha activity. NeuroImage 2003a;19(4):1463–76.

Laufs H, Krakow K, Sterzer P, Eger E, Beyerle A, Salek-Haddadi A, et al. Electroencephalographic signatures of attentional and cognitive default modes in spontaneous brain activity fluctuations at rest. Proc Natl Acad Sci U S A. 2003b;100(19):11053–8.

Laufs H, Walker MC, Lund TE. 'Brain activation and hypothalamic functional connectivity during human non-rapid eye movement sleep: an EEG/fMRI study'–its limitations and an alternative approach. Brain 2007;130:e75. author reply e76.

Lopes da Silva FH, Hoeks A, Smits H, Zetterberg LH. Model of brain rhythmic activity. Kybernetik 1974;15(1):27–37.

Lopez-Serna R, Gonzalez-Carmona P, Lopez-Martinez M. Bilateral thalamic stroke due to occlusion of the artery of Percheron in a patient with patent foramen ovale: a case report. J Med Case Rep 2009;3:7392.

Lund TE, Madsen KH, Sidaros K, Luo W-L, Nichols TE. Non-white noise in fMRI: does modelling have an impact? NeuroImage 2006;29(1):54–66.

Maquet P. The role of sleep in learning and memory. Science 2001;294(5544):1048–52.

Moosmann M, Ritter P, Krastel I, Brink A, Thees S, Blankenburg F, et al. Correlates of alpha rhythm in functional magnetic resonance imaging and near infrared spectroscopy. NeuroImage 2003;20(1):145–58.

Olbrich S, Mulert C, Karch S, Trenner M, Leicht G, Pogarell O, et al. EEG-vigilance and BOLD effect during simultaneous EEG/fMRI measurement. NeuroImage 2009;45(2):319–32.

Pfurtscheller G, Stancák A, Neuper C. Event-related synchronization (ERS) in the alpha band — an electrophysiological correlate of cortical idling: A review. Int J Psychophysiol 1996;24(1–2):39–46.

Picchioni D, Fukunaga M, Carr WS, Braun AR, Balkin TJ, Duyn JH, et al. fMRI differences between early and late stage-1 sleep. Neurosci Lett 2008;441(1):81–5.

Plihal W, Born J. Effects of early and late nocturnal sleep on declarative and procedural memory. J Cogn Neurosci 1997;9(4):534–47.

Rechtschaffen A. A manual of standardized terminology, techniques and scoring system for sleep stages of human subjects. Bethesda MD: U.S. Dept. of Health Education and Welfare Public Health Services-National Institutes of Health National Institute of Neurological Diseases and Blindness Neurological Information Network; 1968.

Sadaghiani S, Scheeringa R, Lehongre K, Morillon B, Giraud A-L, Kleinschmidt A. Intrinsic connectivity networks, alpha oscillations, and tonic alertness: a simultaneous electroencephalography/functional magnetic resonance imaging study. J Neurosci 2010;30(30):10243–50.

Scheeringa R, Petersson KM, Kleinschmidt A, Jensen O, Bastiaansen MCM. EEG alpha power modulation of fMRI resting-state connectivity. Brain Connect 2012;2(5):254–64.

Seeley WW, Menon V, Schatzberg AF, Keller J, Glover GH, Kenna H, et al. Dissociable intrinsic connectivity networks for salience processing and executive control. J Neurosci. 2007;27(9):2349–56.

Tagliazucchi E, Laufs H. Decoding wakefulness levels from typical fMRI resting-state data reveals reliable drifts between wakefulness and sleep. Neuron 2014;82(3):695–708.

Tagliazucchi E, von Wegner F, Morzelewski A, Brodbeck V, Laufs H. Dynamic BOLD functional connectivity in humans and its electrophysiological correlates. Front Hum Neurosci 2012;6:339.

Tinguely G, Finelli LA, Landolt H-P, Borbely AA, Achermann P. Functional EEG topography in sleep and waking: state-dependent and state-independent features. NeuroImage 2006;32(1):283–92.

Torrence C, Compo GP. A practical guide to wavelet analysis. Bull Am Meteorol Soc 1998;79:61–78.

Valdes PA, Jimenez JC, Riera J, Biscay R, Ozaki T. Nonlinear EEG analysis based on a neural mass model. Biol Cybern. 1999;81(5–6):415–24.

von Wegner F, Tagliazucchi E, Brodbeck V, Laufs H. Analytical and empirical fluctuation functions of the EEG microstate random walk - Short-range vs. long-range correlations. Neuroimage 2016;141:442–51.

Weyand TG, Boudreaux M, Guido W. Burst and tonic response modes in thalamic neurons during sleep and wakefulness. J Neurophysiol 2001;85(3):1107–18.

Wright Jr KP, Badia P, Wauquier A. Topographical and temporal patterns of brain activity during the transition from wakefulness to sleep. Sleep 1995;18(10):880–9.